



Thermal performances of a small-scale salt gradient solar pond under Moroccan climate

A. El Mansouri^{1,2}, M. Hasnaoui¹, R. Bennacer² and A. Amahmid¹

¹UCA, Faculty of Sciences Semlalia, Physics Department, LMFE, Unit affiliated to CNRST (URAC 27), BP 2390, Marrakech, Morocco

²ENS Paris-Saclay Dpt GC/LMT, 61, Av du Président Wilson 94235 Cachan Cedex France

^{1,2}*abdelfattah.elmansouri@edu.uca.ac.ma*, ¹*hasnaoui@uca.ac.ma*, ²*rbennace@ens-cachan.fr*,
¹*amahmid@uca.ac.ma*

Abstract: A two-dimensional numerical study is conducted to investigate quantitatively and qualitatively the thermal characteristics of a small-scale salt gradient solar pond (SGSP) operating under real climate weather. A realistic model was formulated based on the Navier-Stokes equations and the energy and salt transport equations. The developed model ensures a suitable treatment of the boundary conditions especially at the free surface of the pond in contact with the ambiance and considers the internal heating engendered by the absorption of solar radiation. This model was solved using a numerical tool based on the Finite-Volume and Lattice-Boltzmann hybrid scheme. After five days from the start of the heating process of the pond, the operating temperature in the heat storage zone has increased from 25 °C to reach 49.3 °C and the energy stored in this zone has slightly exceeded 40 MJ. The storage daily efficiency of the SGSP is seen to vary in the range from 25.62 % to 36.51 %. Obviously, these preliminary outcomes demonstrate the important storage potential of the SGSP.

Key words: Solar ponds, Heat storage, Solar radiation absorption.

1. Introduction

Solar ponds are pools of water that allow caption and storage of incident solar radiation. Salt gradient solar ponds are the most popular among other types of existing solar ponds. Basically, they are constituted of three horizontal layers, each of them is characterized by its own salinity and thickness. Such solar ponds have attracted the attention of researchers over the past few decades. This interest stems from their important capacity of thermal energy storage. In addition, most of the technologies are actually progressively oriented towards the use of renewable energy instead of fuel whose price is not stable and very dependent on the geo-political stakes. The literature review shows that the research efforts have been mainly devoted to study the thermal performance and stability of SGSP. Mathematical models and numerical methods have been developed to simulate solar ponds working under real conditions but also under some assumptions (like 1D model) to alleviate the computational effort. Some experimental attempts have been carried out using small reservoirs or mini-basins. Through the last fifteen years, Akbarzadeh and his collaborators [1-3] have contributed by some studies with the aim to determine optimal conditions leading to the improvement of the SGSP thermal efficiency. Their numerical [1, 2] and experimental [3] works focused on an alternative method of heat extraction from the intermediate layer. The outcomes revealed that thermal efficiency of the SGSP can be raised up to 55% by turning heat draw location from the heat storage zone to the intermediate zone using in-pond heat exchangers. Other studies have focused on the examination of the performance of hybrid systems combining SGSP either with a thermodynamic power cycle for water pumping [4], or with a chimney operating as a turbine for power production [5]. In the same spirit, Angeli and Leonardi [6] developed a one-dimensional transient mathematical model allowing a parametric study that demonstrates the important influence of the intermediate zone thickness in increasing the storage temperature. Besides, Karakilcik et al. [7] have investigated the shading effects on energy efficiency of SGSP. Such a study is certainly meaningful in relatively small solar ponds where a significant deterioration of the thermal efficiency ranging from 37.25 % to almost 28 % in the heat storage zone was reported by the authors. However, for large scale solar ponds, where the shaded parts near borders are negligible compared to the total area, this shading effect was found to be negligible. From their part, Sakhrieh and Al-Salaymeh [8] realized a small prototype of solar pond

and compared the recorded temperatures with those obtained numerically. These comparisons have led to a very satisfactory agreement. Despite the small-scale of the prototype, a maximum temperature of 47 °C was reached in the heat storage zone in the spring season. Other works are available in the literature based on both theoretical and experimental approaches. Some non-dimensional studies have considered these assumptions but in a far smaller scale that corresponds to solar ponds of a few millimeters. Most of the theoretical studies were conducted with various simplified models using either one-dimensional approach (only the energy equation is solved) or considering 2D models but neglecting the double-diffusive convection, particularly in the upper and lower convective zones. To the best of the authors' knowledge, only Suárez et al. [9] have addressed numerically the solar pond problem in a real scale using a commercial code. For a better understanding of the two-dimensional effects (a more accurate approach of the solar ponds problem), we have developed a realistic numerical model to assess the thermal characteristics and energy efficiency of a SGSP. Rabel and Nielson's model [10] was implemented to evaluate the internal heating induced by the absorption of solar radiation through the fluid layer of the pond. This model was solved by using a hybrid scheme combining Lattice-Boltzmann method, for density and fluid velocity calculation, with a Finite-Volume method for tackling the fields of temperature and salt concentration. In the present study, we have performed a simulation on a reduced scale of SGSP and the simulations cover five days of summer time under Marrakesh (Morocco) weather conditions. The results are presented in terms of temperature distribution in the pond and energy efficiency throughout the simulation period.

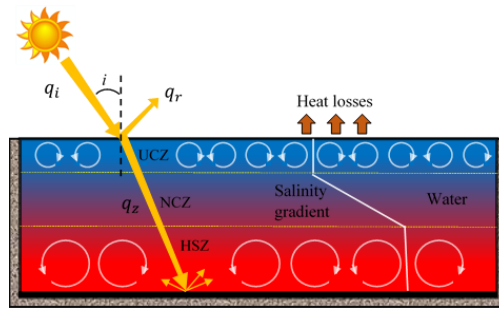


Figure 1. Schematic of a salt gradient solar pond

2. Description of the problem and methodology

2.1. Physical problem

The studied SGSP is sketched in figure 1. It consists of a rectangular open cavity filled with saline water. The initially vertical distribution of salt concentration is dispersed differently on three distinct layers. The lower one (Heat Storage Zone: HSZ) is 40 cm thick and contains brine water at a homogenous salt concentration of 25 %. The upper one (Upper Convective Zone: UCZ) is 20 cm thick and contains fresh water at a uniform low salt concentration of 5 %. A downward increasing salt gradient is imposed in the intermediate zone (Non-Convective Zone: NCZ) where the concentration increases linearly from 5 % at the interface UCZ-NCZ to 25 % at the interface HSZ-NCZ. Equations 1-4 were used to predict the behavior of the SGSP for the five days of Marrakesh summer climate, during which the pond was exposed to actual climate data. These equations are coupled by the fluid density which is supposed to vary linearly with temperature and concentration as indicated by Eq. 5. The free surface of the pond is expected to remain at a constant level since the rate of water evaporation is negligible. The fluid at the free surface constantly interacts with the ambience by exchanging heat under three specific forms: convective or sensible heat, evaporative or latent heat and long-wave radiation heat. The estimation of these three components, predominantly driven by the temperature difference and wind velocity, is handled separately by using available correlations from the literature [11, 12, 13]. The solar radiation penetrating the pond through its free surface is gradually absorbed in the vertical fluid layers and engenders an internal heating of the latter. This process was modeled here in order to compute the source term appearing in Eq. (3) using the four-exponential empirical formulation proposed by Rabel and Nielson [10]. The transient governing equations in their dimensional forms and the fluid density are as follows:

$$\text{Continuity equation:} \quad \frac{\partial \rho}{\partial t} + \text{div}(\rho V) = 0 \quad (1)$$

$$\text{Momentum equation:} \quad \frac{\partial(\rho V)}{\partial t} + \nabla \cdot (\rho V V) = -\nabla P + \mu \Delta V + \rho g \quad (2)$$

Energy equation:
$$\rho_0 C_p \left(\frac{\partial T}{\partial t} + V \cdot \nabla T \right) = \nabla \cdot (k \nabla T) + S_a \quad (3)$$

Salt concentration equation:
$$\frac{\partial(C)}{\partial t} + \nabla \cdot (VC) = \nabla \cdot (D \nabla C) \quad (4)$$

Fluid density:
$$\rho = \rho_0 (1 - \beta_T (T - T_0) + \beta_C (C - C_0)) \quad (5)$$

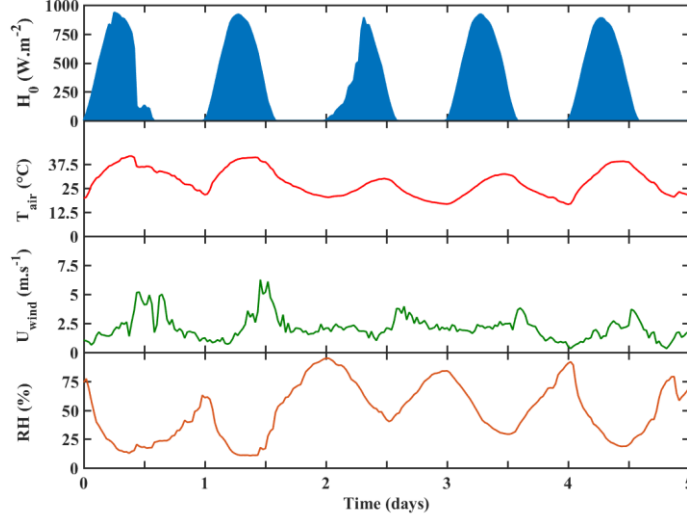


Figure 2. Marrakesh Meteorological data for the period starting from July 1, 2011 at 6:00 am to July 6, 2011 at 6:00 am.

The model briefly described above was used to simulate 1 m^3 of SGSP, subject to the climatic conditions displayed in figure 2. This figure shows from top to bottom temporal variations of the global short-wave radiation, the ambient temperature, the wind speed and the relative humidity for the first five days of July, 2011. The input of these data in the numerical code was updated each thirty minutes.

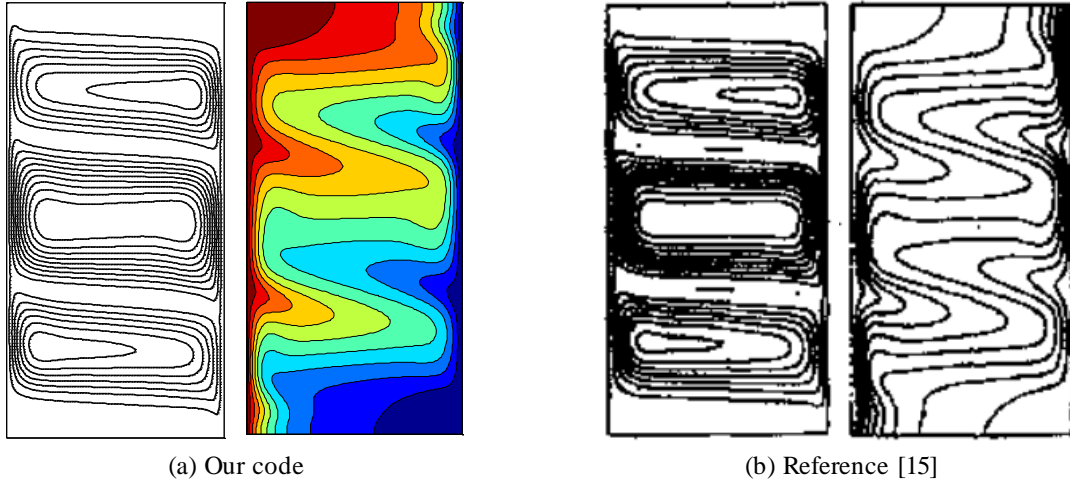


Figure 3. Comparative results in terms of streamlines and isotherms obtained for $Ra_T = 2.8 \times 10^6$, $Ra_S = 5.6 \times 10^7$, $Le = 100$ and $Pr = 7$.

2.2. Methodology and validation

The simulations were carried out using a homemade code based on the lattice-Boltzmann method and allowing the calculation of the density and fluid velocity within the fluid domain. The buoyancy force was carefully implemented by considering the scheme proposed by Guo [14] as the density varies spatially in the computational domain due to the salt concentration distribution. Once calculated, the obtained velocity field is transformed from the Lattice-Boltzmann scale into the real scale before using it to compute the temperature and salt concentration

fields. The latter were calculated by the Finite-Volume approach with high order schemes of discretization. Also, the Alternating Direction Implicit method has been selected to perform the temporal integration. Moreover, in order to assess the ability of our code in describing accurately the physics of a SGSP, two important tests of validation have been carried out. Firstly, we reproduced the results obtained by Gobin et al. [15] in the case of thermosolutal convection induced by horizontal temperature and concentration gradients inside a rectangular cavity. This basic problem is a typical test for the coupled transport phenomenon occurring in a SGSP since the Prandtl and Lewis numbers are respectively 7 and 100. Comparative results presented in Fig. 3 in terms of streamlines and isotherms show that the agreement is excellent. In particular, the multicellular nature of the flow is faithfully reproduced. As complementary tests of validation, we have confirmed the ability of the absorption model adopted here to reproduce experimental and numerical results [9] obtained in a small water lake and presented in Fig. 4 in terms of temporal variations of temperature at a given depth. It can be observed from Fig. 4 that the general trend of the reference experimental curve is realistically reproduced; the maximum difference observed at the considered depth is of about 1 °C.

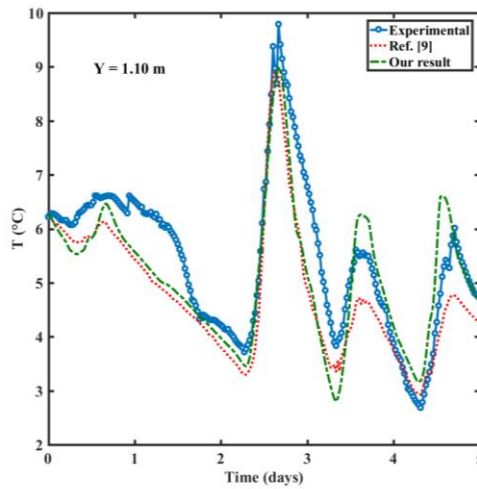


Figure 4. Validation in terms of temperature variations due to solar radiation absorption.

3. Results and discussion

In this section, we analyze both temperature distribution in the SGSP and energy storage efficiency during the five selected days. As mentioned before, the transmitted solar radiation is progressively absorbed between the free surface and the bottom of the pond. It is important to underline that, for a pond one meter deep, almost 36 % of the solar radiation transmitted through the free surface reaches its blackened bottom. In addition, a small amount of heat of about 2 % is lost to the ground and the largest part of the heat absorbed in the bottom of the pond is transferred to the fluid in the form of sensible heat, leading to a large increase in the temperature of the layers adjacent to the bottom of the pond. Then, the mixing process due to the convective motion of fluid below the intermediate zone (i.e. in the HSZ) tends to homogenize the distribution of the heat in this zone. It should be recalled that salt gradients inhibit convective motions in the NCZ, allowing therefore heat entrapment in the HSZ.

3.1. Temperature variations

Another way to confirm the above observations is clearly supported by the temperature fields in the considered SGSP, presented in Fig. 5 at selected moments (6:00 pm) during the simulation period. Hence, after 36 hours of exposure of the pond to solar radiation, the temperature in the HSZ has increased from 25 °C to reach a maximum of 39.06 °C, which is not too far from 37.28 °C representing the mean temperature of storage at this instant (Fig. 5a). Consequently, the transfer of heat by conduction from the HSZ, in the vertical upward direction, gives rise to vertical thermal gradients in the NCZ, particularly in the region located between $Y = 0.4 m$ and $Y = 0.5 m$ which is located near the interface HSZ-NCZ. During the test period, the mean temperature continues to increase in the HSZ (figure 5b-c) as the amount of cooling process during nocturnal periods is less important than the heat gain during the diurnal periods. More specifically, the absorption of solar radiation has raised the mean storage temperature up to 41.01 °C, 46.69 °C and 50.78 °C after 60, 84, and 108 hours, respectively. Moreover,

the thermal gradients expand progressively with time in the upward direction until the establishment of a linear gradient in the NCZ.

By the end of the diurnal periods (at 6:00 pm), the very small amount of solar radiation still reaching the solar pond has a piddling effect on the fluid heating process nearby the bottom of the pond. The fluid currents due to convection, still active in the HSZ, insure good fluid mixing and thereby leads to a uniformization of the temperature (figure 5). As a result, the strong temperature gradients that could be observed near the pond bottom at noon, disappear at the end of the diurnal periods. These observations are corroborated by the figure 6 that illustrates the temporal variations of the horizontally averaged temperature. After each sunrise, time corresponding to 0, 1, 2, 3 and 4 in Fig. 6, a thermal layer of few centimeters is developed near the bottom of the pond where strong vertical gradients of temperature are formed during the diurnal period. Inside this layer, the heat gained by conduction from the bottom is transferred by natural convection towards the upper colder regions of the HSZ. In the same figure, it can be observed that these gradients vanish during the nocturnal part of each day due to the absence of solar radiation. Furthermore, a close inspection of the horizontal zone located few centimeters above the bottom of the pond in the HSZ, allows to see the existence of horizontal thermal gradients during the diurnal part of each day. This indicates a continuous increase of temperature in this region from sunrise to sunset. The daily average temperature increase recorded here was around 5 °C. During the nocturnal periods, a significant decrease of temperature is observed; cooling expected because of heat losses occurring during night. As mentioned before and emphasized once again by figure 6, vertical thermal gradients are developed near the HSZ-NCZ interface ($Y \cong 0.40 \text{ m}$) and extend over time, tending to invade all the NCZ. In this zone, the isotherms become denser day after day indicating the increase of conductive heat losses from the HSZ to the UCZ, where the variations of the mean temperature are extremely sensitive to the ambient temperature ($Y > 0.80 \text{ m}$). Such behavior is attributed to the pond cooling at its upper surface in contact with the ambient air and supported by the convective movements in the UCZ.

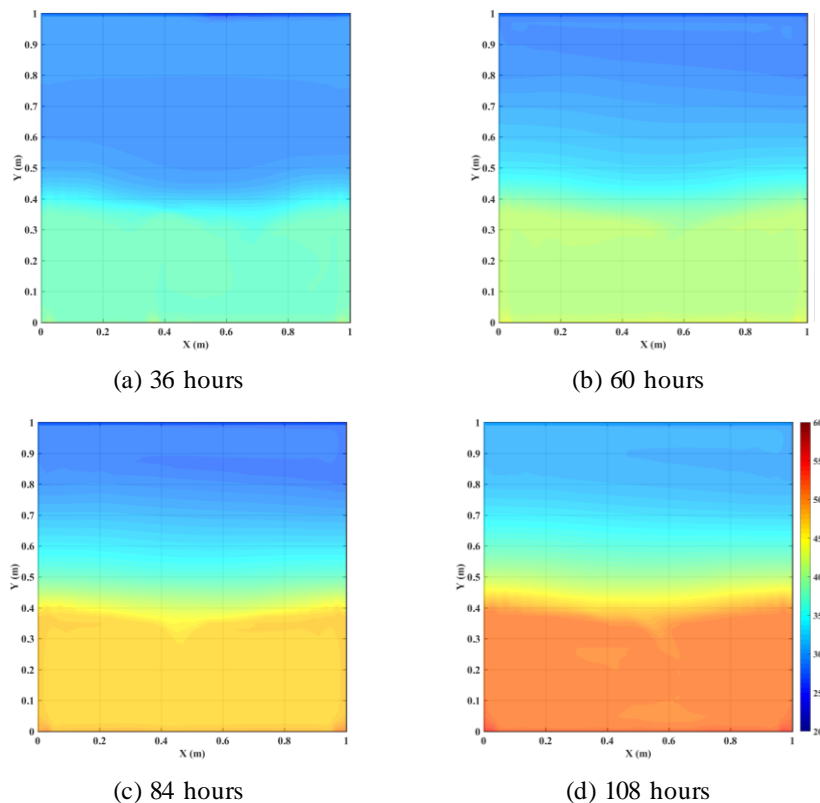


Figure 5. Temperature fields at indicated time from the starting of the simulation

The maximums of mean temperature in the HSZ were recorded at 6:00 pm. Thus, the best moment to extract energy is around this time (6:00 pm). Some researchers have proposed a method of heat extraction from the NCZ as mentioned before in the introduction. Of course, such method can reduce heat losses by retrieving heat on its path towards the free surface and maintains heat trapped in the HSZ. However, the extracted heat may not be of the required quality since this method of extraction allows the access to weak temperatures of draw (mean temperature in the NCZ). For instance, according to the results of simulations obtained at the end of the fifth day,

the considered SGSP can provide heat exchangers with water at the temperatures 38 °C and 50.78 °C respectively from the NCZ and the HSZ.

3.2. Energy storage and efficiency

Given the fact that no heat extraction is envisaged during the simulated period, the overall energy accumulated in the HSZ continues to increase day by day. The amplitudes of the sudden jumps of the energy stored, observed in figure 7, are directly related to the available solar radiation for a given day, and correspond to a new heat reception phase. Besides, the weakness of the heat loss process at the free surface in these periods, due to the high ambient temperature, also favours heat accumulation in the pond. Once the sun sets, the drop of the ambient temperature enhances heat losses through the air-water interface, and then the conductive heat zone is extended at the upper part of the HSZ towards the UCZ. Figure 7 shows that the sudden drops of the energy stored, remain smaller than the precedent diurnal heat gains. In fact, the decrease in the difference of temperature between the water surface and the ambience, in addition to the nocturnal increase of the atmospheric relative humidity, minimize the amount of heat lost during the second part of the night. Furthermore, about forty mega joules (40 MJ) have been stored at the end of the simulations only in the HSZ. The storage daily efficiency in the HSZ presented in the same figure varies in the range between 25.62 % and 36.51 %. The high efficiency observed during the first two days is obviously attributed to the high amounts of energy stored. On the contrary, the minimum storage efficiency of the last day is explained by the small jump of the amount of energy stored. In fact, the relative limited jump compared to the total heat stored during the precedent days is a consequence of the improvement of the conductive heat transfer role between the HSZ and the UCZ in comparison with the previous days (see Fig. 6). The daily efficiency of storage for the third day remains comparable with those of the previous days even if the amount of energy stored is comparable to that of the last day. This is because the energy input due to solar radiations for the third day (see Fig. 2) is less important.

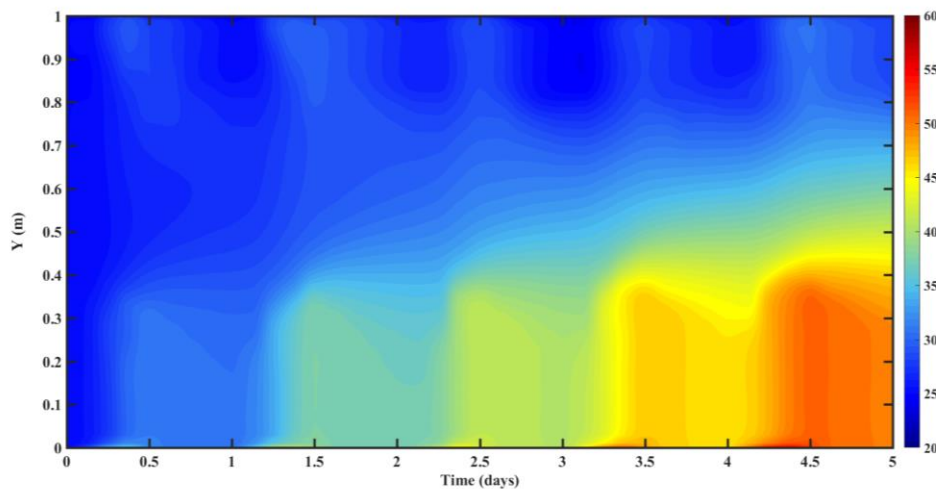


Figure 6. Temporal variations of the vertical profile of temperature during the simulation period.

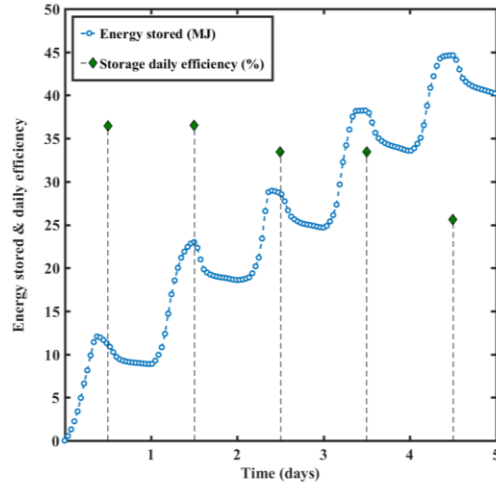


Figure 7. Energy accumulation over time in the HSZ and the storage daily efficiency.

Conclusion

In this numerical study, we have focused on the thermal performances of a small scale SGSP exposed to real weather conditions during five days. The results presented indicate that, despite the fact that the simulations cover only a period of 5 days, the temperature has reached a value around 50 °C in the HSZ and the daily efficiency of storage oscillates around 30 %. The main concluding recommendation based on the current outcomes, is that SGSP at large scale is expected to supply heat for various applications such as in agricultural and agri-foods sectors, in addition to hot water for domestic use.

Nomenclature

Symbol

k	thermal conductivity, $W/(m.K)$
T	temperature, K
T	salt concentration, K
V	fluid velocity, $m.s^{-1}$
P	fluid pressure, Pa
g	gravity acceleration, $m.s^{-2}$

Greek symbols

α	thermal diffusivity, $m^2.s^{-1}$
ρ	fluid density, $kg.m^{-3}$
μ	dynamic viscosity, $kg.(m.s)^{-1}$
β	expansion coefficient
index	
0	reference state
T	thermal
C	Solutal
a	absorption

References

- [1] J. Andrew and A. Akbarzadeh, Enhancing the thermal efficiency of solar ponds by extracting heat from the gradient layer, *Solar Energy*, volume 78, pages 704-716, 2005.
- [2] A. Date, Y. Yaakob, A. Date, S. Krishnapillai and A. Akbarzadeh, Heat extraction from Non-Convective and Lower Convective Zones of the solar pond: A transient study, *Solar Energy*, volume 97, pages 517-528, 2013.
- [3] J. Leblanc, A. Akbarzadeh, J. Andrews, H. Lu and P. Golding, Heat extraction methods from salinity-gradient solar ponds and introduction of a novel system of heat extraction for improved efficiency, *Solar Energy*, volume 85, pages 3103-3142, 2011.
- [4] A. Akbarzadeh and A. Date, Theoretical study of a new thermodynamic power cycle for thermal water pumping application and its prospects when coupled to a solar pond, *Applied Thermal Engineering*, volume 58, pages 511-521, 2013.

- [5] A. Akbarzadeh, P. Johnson and R. Singh, Examining potential benefits of combining a chimney with a salinity gradient solar pond for production of power in salt affected areas, *Solar Energy*, volume 83, pages 1345-1359, 2009.
- [6] C. Angeli and E. Leonardi, A one-dimensional numerical study of the salt diffusion in a salinity-gradient solar pond, *International Journal of Heat and Mass Transfer*, volume 47, pages 1-10, 2004.
- [7] M. Karakilcik, I. Dincer, I. Bozkurt and A. Atiz, Performance assessment of a solar pond with and without shading effect, *Energy Conversion and Management*, volume 65, pages 98-107, 2013.
- [8] A. Sakhrieh and A. Al-Salaymeh, Experimental and numerical investigation of salt gradient solar pond under Jordanian climate conditions, *Energy Conversion and Management*, volume 65, pages 725-728, 2013.
- [9] F. Suárez, S. W. Tyler and A. E. Childress, A fully coupled, transient double-diffusive convective model for salt gradient solar ponds, *International Journal of Heat and Mass Transfer*, volume 53, pages 1718-1730, 2010.
- [10] A. Rabl and C. E. Nielson, Solar ponds for space heating, *Solar Energy*, volume 17, pages 1-12, 1974.
- [11] J. J. Fritz, D. D. Meredith and A. C. Middleton, Non-steady state bulk temperature determination for stabilization ponds, *Water Research*, volume 14, pages 413-420, 1979.
- [12] P. J. Ryan, D. R. F. Harleman and K. D. Stolzenbach, Surface heat loss from cooling ponds, *Water resources research*, volume 10, n° 15, pages 930-938, 1974.
- [13] R. W. Troxler and E. L. Thrackston, Predicting the rate of warming of rivers below hydroelectric installations, *Journal of the Water Pollution Control Federation*, volume 49, pages 1902-1912, 1977.
- [14] Z. Guo, C. Zheng and B. Shi, Discrete lattice effects on the forcing term in the lattice Boltzmann method, *Physical Review E*, volume 65, pages 046308, 2002.
- [15] D. Gobin and R. Bennacer, Cooperating thermosolutal convection in enclosures-II. Heat transfer and flow structure, *International Journal of Heat and Mass transfer*, volume 39, n° 113, pages 2683-2697, 1996.

25-27 Octobre 2017
Monastir - Tunisie